Experimental and Numerical Modelling of the Bombora Wave Energy Converter

Cam Algie [#1], Alan Fleming [*2], Shawn Ryan [#3]

[#]*Bombora Wave Power*
Suite 1, Office 6, Enterprise Unit 3, 9 De Laeter Way, Bentley WA 6102, Australia
[1]cam.algie@bomborawavepower.com.au
[3]shawn.ryan@bomborawavepower.com.au
[*]*University of Tasmania, Australian Maritime College*
Launceston Campus, Maritime Way, Newnham, TAS 7248, Australia
[2]alan.fleming@utas.edu.au

Abstract— **Fast and accurate numerical modelling of wave energy converters (WECs) is critical to cost effective development of these technologies. With the assistance of Applied Renewables Research Ltd., Bombora Wave Power has developed a linear numerical performance modelling suite for their flexible membrane WEC (mWave). For the purpose of numerical model validation, tank testing of a 1:15 scale physical model of this device was conducted at the Australian Maritime College. The numerical model predictions were compared against measured data for 115 monochromatic wave tank-tests. The expected linearity of test waves was estimated by the Ursell parameter. For near-linear waves, phase-averaged time series data was found to agree very well with model pressure and flow predictions. The numerical model also provides a good indication of performance for highly non-linear waves accross a broad range of water depths, wave frequencies and wave heights.**

Keywords— **Wave energy converter, numerical modelling, tank-testing, membrane, validation.**

I. Introduction

The use of deformable structures as the working surface in a wave energy converter (WEC) is being explored by both commercial and academic organisations [1], [2], [3]. Energy conversion is achieved by the coupling of wave forces with the working surface's motion. Increasing conversion performance bandwidth is an important step towards a WEC design that has a commercially viable cost of energy. At a particular frequency, the degree of coupling between wave force and WEC motion is sensitive to the mass associated with the working surface and to its geometry. When compared to the typical rigid structures used as working surfaces in many WEC designs, deformable structures such as membranes have lower inertia and consequently, can be expected to couple effectively with wave forces across a broader range of frequencies [3]. While oscillating water column (OWC) WECs use no structure at all for the working surface, the mass of the enclosed water column means that these designs also have high inertia.

Although strong wave force coupling is desirable for energy conversion, in extreme waves this can become destructive. By definition, deformable structures are capable of large changes in geometry. This feature can be used to modify the degree of exposure to extreme wave forces in storm conditions for WEC survival.

With the aim of exploiting these features, Bombora Wave Power (Bombora) has developed a novel membrane WEC design (*mWave*) comprising multiple seafloor-mounted, air-filled membranes, enclosing discrete air cells (Fig.1a). These cell membranes convert wave forces into internal cell air pressure. Wave peaks and troughs above the WEC cause differential pressure between cells. At any instant, those cells with a higher pressure supply air to the high-pressure manifold via a set of non-return outlet valves. This high pressure air flows through the turbine and returns to low pressure cells, via a low-pressure manifold and non-return inlet valves [1]. The flow circuit is shown in Fig. 1b.

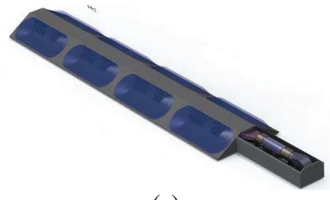

(a)

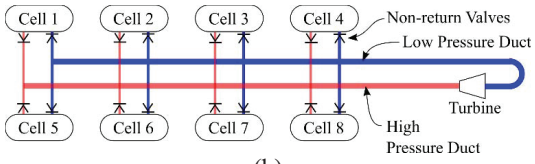

(b)

Fig. 1 The Bombora WEC shown (a) as a CAD render of the full-scale design basis and (b) as a schematic diagram. This design features two parallel banks of cells.

The hydrodynamics of the Bombora WEC are relatively complex due to the interaction between the deformable membrane and the fluid. In addition, the complete system has many degrees of freedom, proportional to the number of cells

ISBN: 978-981-11-0782-5 :: doi:10.3850/978-981-11-0782-5_280 ::

it comprises. No existing numerical tool was capable of modelling the complete system for investigation of performance. Therefore, customised numerical modelling was necessary.

Bombora has undertaken the development of both a non-linear and linear numerical performance model for this purpose. The non-linear model is still in development with the assistance of the Fluid Dynamics Research Group of Curtin University. This model fully couples the WEC membrane motion with the fluid domain of a computation fluid dynamics model. The high computational cost of this method makes the non-linear model unsuitable for anything other than detailed studies. In contrast, the linear model has very low computational cost, and is therefore intended as the primary design tool. The linear model has been developed with the assistance of Applied Renewables Research Ltd. and allows annual energy production prediction and parametric studies of performance for design optimisation.

Here we describe the validation of the linear numerical model by physical model tank-testing undertaken in collaboration with the Australian Maritime College. The primary objective of this work was to estimate the numerical model accuracy for both near-linear and non-linear regular wave conditions.

II. Tank Testing

Testing of a 1:15 scale physical model was conducted by Bombora and the Australian Maritime College (AMC) in the AMC Model Test Basin in Launceston, Tasmania.

To simplify the physical model, a single bank of cells was built. The total membrane length was 4.4m, divided into 12 cells by deformable internal membrane walls, as shown in Fig. 2.

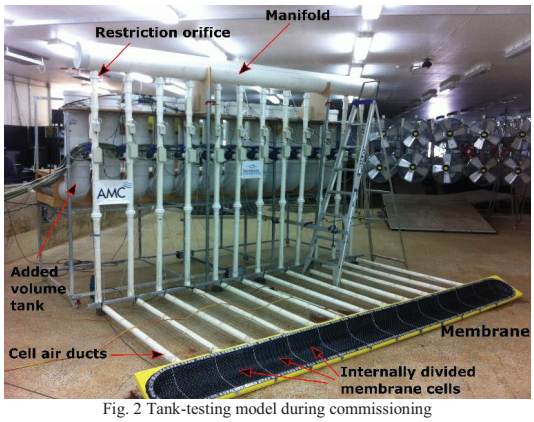

Fig. 2 Tank-testing model during commissioning

The full-scale PTO system was substituted with that shown schematically in Fig. 3. The fully rectified flow circuit was replaced with a common 225mm diameter manifold with which bi-directional flow from each cell communicated via its own smaller 53mm diameter duct and 25mm diameter square-edged restriction orifice. The use of bi-directional orifices to represent the pressure drops associated with the valves and turbine of the full scale system preserves much of this system's damping characteristic while eliminating the need to build a rectified flow circuit with customised valves and a turbine.

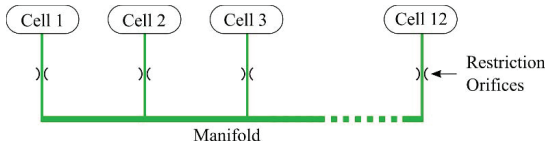

Fig. 3 Schematic diagram of the simplified tank-testing model in which bidirectional cell flow is damped by restriction orifices

The restriction orifices were located above water for access during testing. An added-volume tank (visible in Fig. 2) was connected to each cell duct during all the experiments reported here, to more closely reproduce the relative air spring stiffness of a full scale system.

This model was tested in a 35m by 12m tank, positioned 10m from the wave-maker and 3.6m from the nearest wall, with the membrane at an angle of 45 degrees to the wave crest. The membrane was 50% inflated so that all cells were able to inhale and exhale equally. Testing was conducted at water depths (h) of 0.33m, 0.52m and 0.72m, for a range of regular wave frequencies (f) between 0.21Hz and 0.60Hz with wave heights (H) of between 0.033m and 0.200m. This produced wavelength to depth ratios (λ/h) in the range of 5 to 26, according to linear theory. That is, most waves are of intermediate depth, with only the lowest frequency, lowest depth waves meeting the shallow water definition.

Measured variables included cell pressure, volumetric flow rate in cell ducts, and manifold pressure. Free surface elevations were recorded by conductivity wave probes adjacent to the model. Data was recorded at a rate of 200Hz using a PC fitted with a 16Bit National Instruments PCI card (NI PCI-6254) and USB2 hub. Data was sourced from a range of digital and analogue devices.

Phase averaging of all data was performed using a common phase-signal sourced from either a wave probe positioned adjacent to cell one or from mean manifold pressure. The phase-averaging methods used are described in [4]. Due to the non-linearity of some of the waves tested, the most robust method of phase detection was to use a wavelet based peak detection algorithm. The phase is then allocated on a peak to peak basis.

III. Wave Linearity and Quality

The range of wave parameters tested was selected to be representative of scaled deployment conditions, not to provide waves that fall within the range of validity for linear theory, or within the calibrated range for the wave-maker. Therefore, many of the test waves were not expected to maintain a linear profile, regardless of how they were generated.

Ursell's parameter can be used to quantify the analytically valid range of linear theory in terms of wave height, wavelength and depth, so that $Ur = H\lambda^2/(2h^3)$. Linear theory is

considered analytically valid for $Ur \ll O(0)$ [5]. In shallow water, waves are best described as linear shallow water waves when $Ur \ll O(1)$, cnoidal or solitary waves when $Ur = O(1)$ and non-linear shallow water waves when $Ur \gg O(1)$ [6].

A plot of the Ursell parameter for the range of wave-maker input parameters used in the tank testing (Fig. 4) shows that a broad range of linearity can be expected. Only the shortest period, smallest height waves in depths of 0.52m and 0.72m satisfy the Ursell number limit for linear theory validity. The remaining waves range from solitary/cnoidal through to non-linear (assuming shallow water).

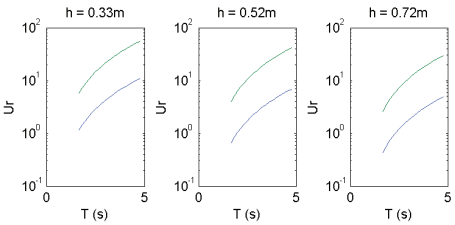

Fig. 4 Plot of Ursell parameter for the range of wave heights, depths and periods tested. Green: Maximum wave height tested. Blue: Minimum wave height tested.

Experimental wave quality was assessed by removing the model from the tank and measuring wave height at the cell locations. This data was used to assess wave profile linearity, wave height spatial homogeneity, agreement with wave-maker input wave parameters and agreement with linear wave theory predictions of relative wave phase across the model. As expected, a broad range of wave quality was found, particularly with respect to spatial homogeneity of wave height. A maximum variation of 19% in wave height across cell position was observed. This variability was not consistent between tests.

Figure 5 shows qualitatively the general correlation between the linearity of the wave profile measured during tank-tests, and the Ursell parameter calculated using wave-maker input parameters. These calculations assume wavelengths calculated from the input wave period, water depth and linear theory. The lowest Ursell parameter corresponds to a highly linear profile. As the Ursell parameter increases, linearity clearly decreases. For the two highest Ursell parameters, secondary wave peaks are observable.

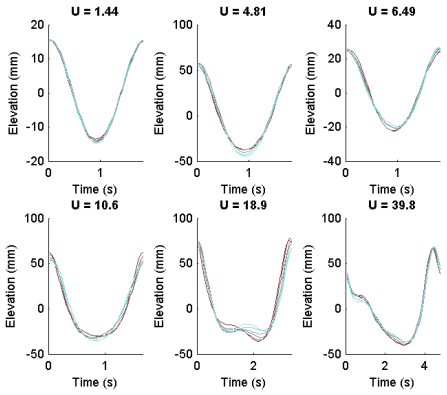

Fig. 5 Phase-averaged wave profiles measured with the model removed from the tank, in descending order of expected linearity according to the Ursell parameter (shown above plot). These are a representative selection of six tests spanning the range of the Ursell parameter tested. For each test, the profile at six locations across the range of cell positions is plotted.

Mostly as a consequence of this non-linearity in wave profiles, agreement between wave measurements and wave-maker inputs was quite variable. Despite this, relative wave phase across cell locations was predicted well by linear theory. The method used to determine an equivalent numerical wave for each simulation is described in Section V.

IV. Numerical Model

The physical system of the tank-test model is divided into three main components for modelling:

1. Hydrodynamics (external side of membrane)
2. Membrane deformation
3. PTO thermodynamics (internal side of membrane)

The hydrodynamic and thermodynamic systems are fully coupled in the numerical model by applying Newton' Second Law to the motion of the cell membranes, so that for a particular cell

$$F_w + F_i + F_k = (M_W^\infty + M_A)\dot{v} \tag{1}$$

where F_w is the total hydrodynamic force on the cell membrane due to the incident wave and the waves generated by the motion of other cell membranes, F_i is the force due to the internal air pressure of the cell and F_k is the force required represent the effect of non-linear membrane hydrostatic stiffness. On the right hand side, M_W^∞ is the added mass coefficient of the water external to the cell membrane (at infinite frequency), M_A is the effective mass of air contained within the 4m cell duct that is accelerating sympathetically with the membrane and $\dot{v}$ is the cell membrane acceleration. The effective air mass is increased by the ratio of membrane area to duct cross section area. Analysis of empirical cell flow rates and pressure differentials between each cell and manifold confirmed that at this scale the effect of air inertia on flow

within the cell ducts was significant. The mass of the membrane itself is neglected, as it is not significant.

Hydrodynamic modelling was conducted using the open-source software NEMOH. This uses the boundary element method to solve the potential flow problem for rigid bodies in linear waves [7]. The use of linear hydrodynamics allows the pre-calculation of hydrodynamic coefficients for the cell membranes and of impulse response functions for the hydrodynamic effect of one cell membrane's motion on another. These calculations assume that each membrane deforms as a scaled mode of a symmetric parabolic shape as shown in Fig. 6. Each cell is assumed to have a membrane that deforms in two dimensions only (x and y in Fig. 6). Cells are divided by an idealised cell wall in the x-y plane. The effect of membrane tension due to unequal deformation of adjacent cells is neglected. At any instant, the membrane is treated as a rigid surface having the shape corresponding to its current deformation mode. The membrane hydro-static stiffness is then modified to have the nonlinear characteristic determined prior by a more detailed study of membrane deformation shape, using a finite element membrane model described in [8].

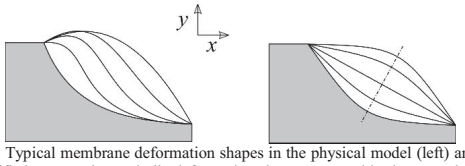

Fig. 6 Typical membrane deformation shapes in the physical model (left) and simplified symmetric parabolic deformation shapes assumed in the numerical performance modelling (right).

The thermodynamic model was adapted to represent the simplified PTO system used in the tank-testing. The orifice loss coefficient, K_L, was estimated from the physical test data ($K_L = 2.65$) and implemented in the model so that $\Delta p = K_L\ (\rho U^2)/2$, where Δp is the pressure drop between cell and manifold, ρ is the air density and U is the mean air velocity.

A total of 50 state equations describe the complete dynamic model in the time domain. These states comprise of air pressure and air mass in each cell and the manifold, and the displacement and velocity of each cell membrane. The mass of air in a cell is defined to include the mass of air in the associated cell duct. The state-space model is solved using an explicit Runge-Kutta solver.

V. Results and Validation

For the validation, a total of 124 tank-tests were completed. Nine of these were discarded, principally due to wave quality issues in those particular tests. The remaining 115 were compared to numerical simulations. Each numerical simulation used linear wave parameter inputs that yielded the same standard deviation in surface elevation as that measured in the corresponding tank test. These input parameters yielded Ursell numbers ranging from 0.4 to 35.

The first part of the study's objective, to estimate the accuracy of the numerical model for near-linear wave conditions, was addressed by a detailed analysis of the results of this comparison for three selected tank-tests. These tests were selected based on the linearity of their wave profile and to provide some range of height, frequency and depth for the comparison. The nominal wave parameters for these three tests are summarised in Table II.

TABLE II
Nominal test parameters

Tank test	Wave height (m)	Wave period (s)	Depth (m)	$Ur = \frac{H\lambda^2}{2h^3}$
C03R324M02	0.167	2.00	0.52	5.2
C03R325M02	0.167	1.67	0.52	3.4
C03R740M02	0.100	2.50	0.72	3.6

Time-averaged cell power and phase-averaged cell pressure and flow were calculated for each test. Analysis results are presented here for the example of tank test C03R324M02. The relative average power capture per cell is presented in Fig. 7 and the phase-averaged cell pressures and flow rates are presented for comparison in Fig. 8. The results of this comparison are typical for the most linear incident waves in tank testing.

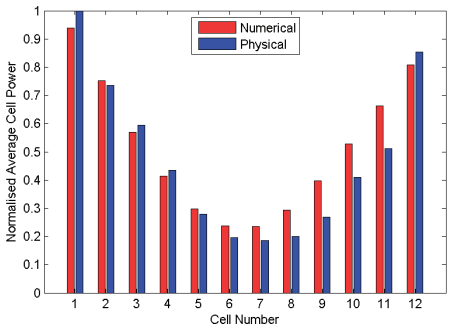

Fig. 7 Normalised average power contributed by each cell in tank-test C03R324M02 and the corresponding numerical simulation.

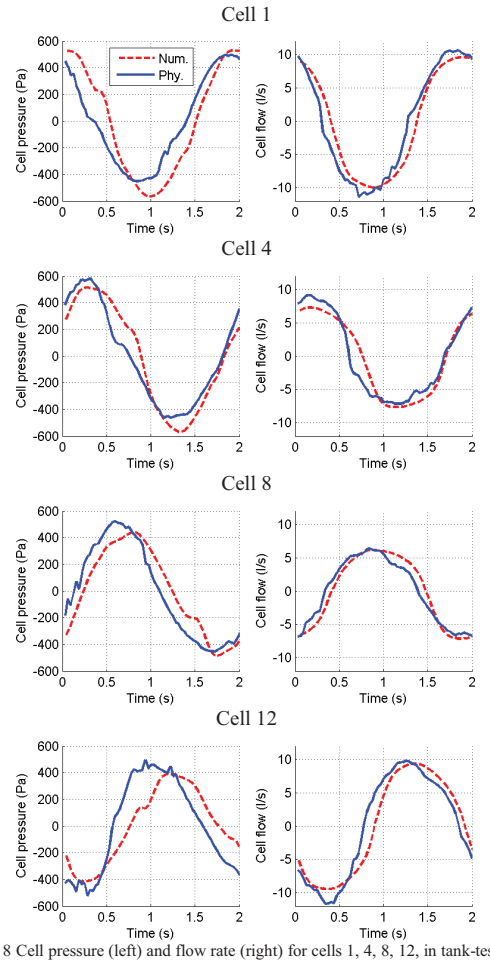

Fig. 8 Cell pressure (left) and flow rate (right) for cells 1, 4, 8, 12, in tank-test C03R324M02 and the corresponding numerical simulation.

The second part of the study's objective, to estimate the accuracy of the numerical model across a broader range of conditions including non-linear waves, was addressed by repeating the comparison of numerical and physical results for all 115 tests from the full validation set. A statistical analysis of the error between numerical and physical results was then conducted.

The magnitude of the oscillatory pressure and flow experienced by each cell can be characterised by the root-mean-square (RMS) of each of these variables within each test. Taking the mean RMS across cells quantifies the change in each of these variables a single value for each test. A comparison of the pressure and flow mean RMS, for the 115 tests, is presented in Fig. 9 and Fig. 10. The numerically predicted cell pressure is observed to agree well with the measured pressure across the full range of validation tests. Cell flow also shows good correlation, however there is a tendency for the numerical model to over-predict the flow for lower flow tests.

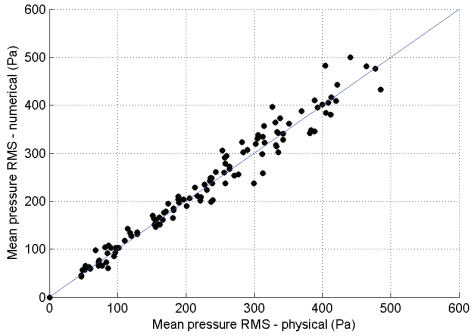

Fig. 9 Comparison of cell pressure RMS, averaged across cells.

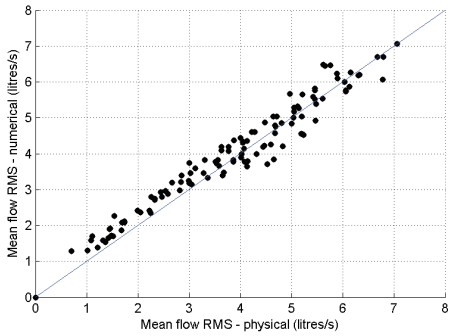

Fig. 10 Comparison of cell flow rate RMS, averaged across cells.

Power capture is defined as the total fluid power observed between the cells and the common manifold. The mean power capture for the complete WEC in each tank test is compared to the numerical model prediction in Fig. 11. This figure shows the same tendency for slight over-prediction of power that was observed for flow, in the lower part of the power range only. Across the remainder of the power range the percentage error is within +/- 40%, with standard deviation of 20% when normalised physical power capture is greater than 0.2.

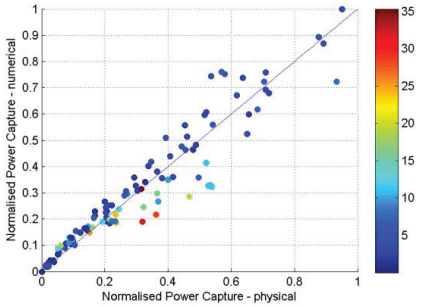

Fig. 11 Comparison of total system power capture, with the wave Ursell parameter indicated by marker colour.

The effect of the Ursell number on the error between numerical and physical power capture was then investigated. For all tests with $Ur < 4$, the standard deviation in percentage error is 17%. This reduces to 12%, when this Ursell limit is applied to tests with a normalised power capture of greater than 0.2. In contrast, for all tests with $Ur > 4$, the standard deviation in percentage error is 30%, and reduces to 22% for normalised power captures of greater than 0.2. These effects can be seen in Fig. 12 which shows a considerably tighter correlation for low Ursell number tests than for high, but a comparable tendency for slight over prediction at low powers.

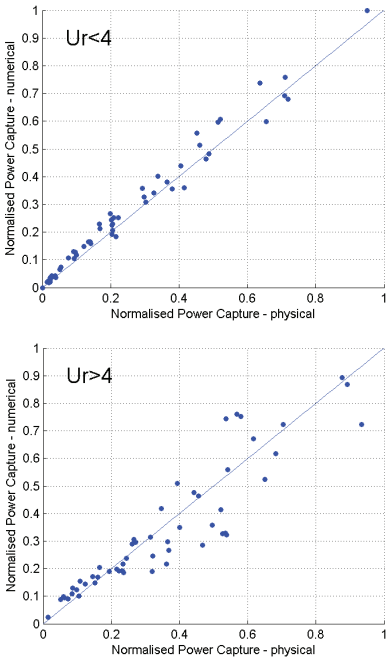

Fig. 12 Comparison of total system power capture for all tests above and below the limit $Ur = 4$

VI. Discussion

The objective of determining the accuracy of the numerical model for near-linear waves was addressed by the detailed analysis of numerical and physical cell pressure, flow and power. This analysis shows that when waves are near-linear, time-averaged cell power capture and phase-averaged cell pressure and flow are predicted well. This is true for all cells, despite a difference of up to 80% in the distribution of power capture across cells in the example presented. These results build confidence that the numerical model is accounting for the physical processes that are most significant in determining WEC performance. They confirm that the modelling of the membrane deformation and thermodynamic system is appropriate.

The objective of determining model accuracy in a broader range of conditions was addressed by statistical comparison of numerical and physical results for all 115 validation tests. This showed that model predictions are reasonably accurate even when non-plane and highly non-linear waves are included (Ursell numbers of up to 35). For the majority of these tests, excluding very low power waves, the standard deviation of model error with respect to measured data is 20%.

When investigated in more detail, wave non-linearity was found to reduce model accuracy as expected. This is reflected in the significantly lower standard deviation in error found when only waves with a low Ursell parameter are considered. The method of matching the standard deviation of surface elevation between tank-test and numerical simulation allows the approximation of measured non-linear waves by linear wave parameters, but does not guarantee the same incident wave energy in each case.

With the known errors in the incident height due to inhomogeneity, and in power due to non-linearity, numerical model accuracy in the broad comparison is as good as can be expected. Assuming these errors are reasonably represented as a standard error in incident wave heights of 10-20%, a standard error of up to 20% in incident wave power is likely. Therefore, it is unreasonable to expect significantly less error in the model predictions than has been found.

The error due to the linear approximation will also affect model accuracy when it is used for full-scale predictions. Therefore, further systematic calibration of the model for the particular non-linear wave forms expected at real sites is recommended to further improve confidence in the model. This calibration can be initially conducted by comparison of the current linear model results with those of the non-linear model under development. Following this intermediate step, final calibration can be made against physical testing at full scale.

The slight over-prediction of flow and power at low levels is a clearly systematic error, making calibration of this relatively straight forward. The most likely cause of this error is the characterisation of the orifices within this range. In addition, measured power capture was observed to achieve small negative values occasionally for some cells. These inconsistencies are believed to indicate complexity in the physical model air flow that has not been accounted for by the numerical model. They are consistent with the effects of air

inertia which, although accounted for in cell ducts, is neglected in the common manifold. Flow within the manifold is complex with multiple alternating bi-directional sources. While this is not a feature of the full-scale PTO, it has other complexities in terms of geometry, valve dynamics and turbine dynamics, all of which require careful implementation.

A significant simplification made in this validation is the inclusion of monochromatic waves only. The numerical model is capable of simulating irregular wave sea-states by the super-position of multiple linear component waves. While validation of the model for these conditions is desirable, this was not feasible with the available facilities. Irregular wave tests require longer durations, which introduce large errors due to reflected waves without a highly effective beach.

However, considerable confidence in the numerical model's predictions for irregular waves is gained from the results for monochromatic waves. The monochromatic results cover a broad range of wave heights and frequencies. The range of these parameters expected to dominate the sea-states of interest has been tested at the model scale. Further, despite the regularity of the incident wave, the system response quickly becomes irregular due to the configuration of multiple cells within the single PTO circuit. Therefore, the only aspect of model performance for irregular waves that is yet to be validated is the hydrodynamic force.

VII. CONCLUSIONS

The numerical model was found to predict power capture across a broad range of wave heights, water depth, wave frequencies and wave linearity. A standard deviation in error of 20% has been estimated. More detailed investigation of model performance with respect to the Ursell parameter indicates that nearly half of this error was the result of non-linearity in incident waves. Slight over prediction of flow and power at low levels demonstrates a need for careful implementation and calibration of any additional PTO model elements required for the full-scale model.

Further work is underway to calibrate the model against CFD results for non-linear wave forces, and to separately validate aspects of the fully-rectified PTO model.

ACKNOWLEDGMENT

Tank-testing data collection and analysis was conducted as an Australian Research Council Linkage Project (110200129) in collaboration with the Australian Maritime College.
Development of the numerical model code and validation of model results were primarily conducted by Dr. Matt Foley of Applied Renewables Research.

REFERENCES

[1] S. Ryan, C.Algie, G. Macfarlane, A. Fleming, I. Penesis and A. King, "The Bombora wave energy converter: A novel multi-purpose device for electricity, coastal protection and surf breaks" in *Australian Coasts & Ports Conference,* 2015: 541-546.

[2] P. M. Koola and A. Ibragimov, "The dynamics of Wave Carpet - a novel deep water wave energy design," *Proceedings OCEANS 2003, San Diego, CA, USA,* 2003, pp. 2288-2293 Vol.4.

[3] A. Kurniawan, D. Greaves and J. Chaplin, "Wave energy devices with compressible volumes." in *Proc. R. Soc. A '14*, 2014, p. 470

[4] A. Fleming, I. Penesis, L. Goldsworthy, G. Macfarlane, Neil B., and T. Denniss. "Phase Averaged Flow Analysis in an Oscillating Water Column Wave Energy Converter." *Journal of Offshore Mechanics and Arctic Engineering* 135, no. 2, 2012.

[5] M. E. McCormick, *Ocean Engineering Mechanics,* New York, USA, Cambridge University Press, 2010.

[6] I. A. Svendsen, *Introduction to Nearshore Hydrodynamics,* Singapore, World Scientific Publishing Co. Pte. Ltd., 2006.

[7] A. Babarit, G. Delhommeau. "Theoretical and numerical aspects of the open source BEM solver NEMOH". *In Proc. of the 11th European Wave and Tidal Energy Conference (EWTEC2015)*, Nantes, France

[8] A. King, C. Algie and S. Ryan, "Modelling of large deformations in membranes for analysis of wave energy converters," in *Proc. Of 3rd Symposium on FSSIC,* 2015, paper.